Semiclassical model for attosecond angular streaking

M. Smolarski,[1,2,*] P. Eckle,[2] U. Keller,[2] and R. Dörner[1]

[1] *Institut für Kernphysik, University Frankfurt, Max-von-Laue Str. 1, D-60438 Frankfurt, Germany*
[2]*Department Physik, ETH Zurich, Wolfgang-Pauli-Str. 16, 8093 Zurich, Switzerland*
**smolarki@phys.ethz.ch*

Abstract: Attosecond angular streaking is a new technique to achieve unsurpassed time accuracy of only a few attoseconds. Recently this has been successfully used to set an upper limit on the electron tunneling delay time in strong laser field ionization. The measurement technique can be modeled with either the time-dependent Schrödinger equation (TDSE) or a more simple semiclassical approach that describes the process in two steps in analogy to the three-step model in high harmonic generation (HHG): step one is the tunnel ionization and step two is the classical motion in the strong laser field. Here we describe in detail a semiclassical model which is based on the ADK theory for the tunneling step, with subsequent classical propagation of the electron in the laser field. We take into account different ellipticities of the laser field and a possible wavelength-dependent ellipticity that is typically observed for pulses in the two-optical-cycle regime. This semiclassical model shows excellent agreement with the experimental result.

OCIS codes: (000.2700) General science.

References and links

1. L. V. Keldysh, "Ionization in the field of a strong electromagnetic wave," Soviet Phys. JETP **20**, 1307 (1965).
2. H. R. Reiss, "Limits on tunneling theories of strong-field ionization," Phys. Rev. Lett. **101**(4), 043002 (2008).
3. P. B. Corkum, "Plasma perspective on strong field multiphoton ionization," Phys. Rev. Lett. **71**(13), 1994–1997 (1993).
4. H. R. Telle, G. Steinmeyer, A. E. Dunlop, J. Stenger, D. H. Sutter, and U. Keller, "Carrier-envelope offset phase control: A novel concept for absolute optical frequency measurement and ultrashort pulse generation," Appl. Phys. B **69**(4), 327–332 (1999).
5. G. G. Paulus, ""A Meter of the "Absolute" Phase of Few-Cycle Laser Pulses," Laser Phys. **15**, 843–854 (2005).
6. P. Dietrich, F. Krausz, and P. B. Corkum, "Determining the absolute carrier phase of a few-cycle laser pulse," Opt. Lett. **25**(1), 16–18 (2000).
7. P. Eckle, M. Smolarski, P. Schlup, J. Biegert, A. Staudte, M. Schöffler, H. G. Muller, R. Dörner, and U. Keller, "Attosecond angular streaking," Nat. Phys. **4**(7), 565–570 (2008).
8. C. Smeenk, L. Arissian, A. Staudte, D. M. Villeneuve, and P. B. Corkum, "Momentum space tomographic imaging of photoelectrons," J. Phys. B **42**(18), 185402 (2009).
9. R. P. Feynman, "Space-Time Approach to Non-Relativistic Quantum Mechanics," Rev. Mod. Phys. **20**(2), 367–387 (1948).
10. P. Salières, B. Carré, L. Le Déroff, F. Grasbon, G. G. Paulus, H. Walther, R. Kopold, W. Becker, D. B. Milosević, A. Sanpera, and M. Lewenstein, "Feynman's path-integral approach for intense-laser-atom interactions," Science **292**(5518), 902–905 (2001).
11. M. V. Ammosov, N. B. Delone, and V. P. Kraĭnov, "Tunnel ionization of complex atoms and of atomic ions in an alternating electromagnetic field," Sov. Phys. JETP **64**, 1191–1194 (1986).
12. T. Gabriel, "Dispersion-Free Reflective Phase Retarder for Few-Cycle Femtosecond Pulses", Paper FB6, Optical Interference Coatings Topical Meeting, Tuscon (AZ), June 6–11 2010.
13. R. Trebino, K. W. DeLong, D. N. Fittinghoff, J. N. Sweetser, M. A. Krumbügel, B. A. Richman, and D. J. Kane, "Measuring ultrashort laser pulses in the time-frequency domain using frequency-resolved optical gating," Rev. Sci. Instrum. **68**(9), 3277–3295 (1997).
14. C. Iaconis, and I. A. Walmsley, "Self-Referencing Spectral Interferometry for Measuring Ultrashort Optical Pulses," IEEE J. Quantum Electron. **35**(4), 501–509 (1999).

#129004 - $15.00 USD Received 25 May 2010; revised 23 Jul 2010; accepted 23 Jul 2010; published 2 Aug 2010

15. M. Nisoli, S. Stagira, S. De Silvestri, O. Svelto, S. Sartania, Z. Cheng, M. Lenzner, C. Spielmann, and F. Krausz, "A novel high-energy pulse compression system: generation of multigigawatt sub-5-fs pulses," Appl. Phys. B **65**(2), 189–196 (1997).
16. C. P. Hauri, W. Kornelis, F. W. Helbing, A. Heinrich, A. Couairon, A. Mysyrowicz, J. Biegert, and U. Keller, "Generation of intense, carrier-envelope phase-locked few-cycle laser pulses through filamentation," Appl. Phys. B **79**(6), 673–677 (2004).
17. G. Szivessy, and C. Münster, "Über die Prüfung der Gitteroptik bei aktiven Kristallen," Ann. Phys. **412**(7), 703–736 (1934).
18. S. C. McClain, L. W. Hillman, and R. A. Chipman, "Polarization ray tracing in anisotropic optically active media. I. Algorithms," J. Opt. Soc. Am. **10**(11), 2371–2382 (1993).
19. S. C. McClain, L. W. Hillman, and R. A. Chipman, "Polarization ray tracing in anisotropic optically active media. II. Theory and physics," J. Opt. Soc. Am. A **10**(11), 2383–2393 (1993).
20. E. D. Palik, "Handbook of Optical Constants of Solids," (Academic Press, 1985).
21. M. J. Dodge, "Refractive properties of magnesium fluoride," Appl. Opt. **23**(12), 1980–1985 (1984).
22. P. Antoine, A. L'Huillier, M. Lewenstein, P. Salières, and B. Carré, "Theory of high-order harmonic generation by an elliptically polarized laser field," Phys. Rev. A **53**(3), 1725–1745 (1996).
23. N. B. Delone, and V. P. Krainov, "Energy and angular electron spectra for the tunnel ionization of atoms by strong low-frequency radiation," J. Opt. Soc. Am. B **8**(6), 1207–1211 (1991).
24. H. R. Schwarz, "Numerische Mathematik," B. G. Teubner, ed. (Verlag, 1997).
25. M. Uiberacker, Th. Uphues, M. Schultze, A. J. Verhoef, V. Yakovlev, M. F. Kling, J. Rauschenberger, N. M. Kabachnik, H. Schröder, M. Lezius, K. L. Kompa, H.-G. Muller, M. J. J. Vrakking, S. Hendel, U. Kleineberg, U. Heinzmann, M. Drescher, and F. Krausz, "Attosecond real-time observation of electron tunnelling in atoms," Nature **446**(7136), 627–632 (2007).
26. C. M. Maharjan, A. S. Alnaser, X. M. Tong, B. Ulrich, P. Ranitovic, S. Ghimire, Z. Chang, I. V. Litvinyuk, and C. L. Cocke, "Momentum imaging of doubly charged ions of Ne and Ar in the sequential ionization region," Phys. Rev. A **72**, 041403(R) (2005)
27. X. M. Tong, and C. D. Lin, "Empirical formula for statistic field ionization rates of atoms and molecules by lasers in the barrier-suppression regime," J. Phys. B **38**(15), 2593–2600 (2005).

1. Introduction and basic background

In the regime of the Keldysh parameter [1] $\gamma \approx 1$ at 800 nm ionization in a strong laser field can successfully be described as a tunneling process [2]. Experimental results show that the pulse shape and helicity of the laser pulse used in the experiment have to be considered in momentum distribution calculations. Here we discuss in some detail the simple semiclassical model used to calculate the momentum distribution in single ionization of helium by elliptically polarized ultrashort intense laser pulses under experimental conditions. In analogy to the three-step model in high harmonic generation [3], attosecond angular streaking can be described in a semiclassical two-step model where first the electron tunnels through a finite potential barrier created by the superposition of the atomic and laser electric fields and then, second, the electron is accelerated classically in the strong laser field.

The electron momentum distribution in ionization of atoms by ultra-short laser pulses contains the information about the carrier envelope offset (CEO) phase of the pulse [4]. This effect is being used by the Stereo-ATI spectrometer [5] to determine the CEO phase of the linearly polarized pulses. The asymmetry of the momentum distribution introduced by CEO-effects is rather small for linearly polarized light unless rescattered, high energy electrons are considered as well [5].

For circularly polarized light a higher contrast for CEO phase measurements was predicted: For short pulses, the theory predicts a strongly peaked momentum distribution in the polarization plane of the pulse, and the continuous rotation of the peak around the origin with changing CEO phase values [6]. However, this simple linear mapping of the CEO phase with the direction of the peak of the electron distribution has never been observed under real experimental conditions. Instead, the measured momentum distribution always shows a two-lobe structure, a clear indication for ellipticity of the light [7,8]. In the one-to-two optical cycle regime, the bandwidth of the pulses becomes so large that no perfect circularly polarized pulse can be generated with a quarter-wave plate. Therefore real pulses always have wavelength-dependent ellipticity that has to be taken into account to estimate the electron angular distributions. Even for small deviations from perfect circular polarization (ellipticity ε

#129004 - $15.00 USD Received 25 May 2010; revised 23 Jul 2010; accepted 23 Jul 2010; published 2 Aug 2010

= 1) we observe a significant effect on the electron distribution in strong field ionization due to the high nonlinearity of the ionization process. Therefore it is essential to characterize carefully the ellipticity in the experiment. The idea of mapping the time of ionization to the final momentum is based on the fact that, in the case of strong laser fields, the wave packet of the ionized electron is moving essentially along its classical trajectory in the laser field. This can be seen most elegantly in the Feynman description of quantum mechanics [9,10] given by Eq. (1):

$$\Psi(x,t) \propto \int Dx\, e^{\frac{i}{\hbar}S} \Psi(x_0,t_0) \quad \text{where S is the classical action:}$$
$$S = \int_{t_0}^{t} \frac{1}{2m} p^2(x(t)) - V(x(t))dt, \tag{1}$$

and Dx represents the integral over all paths from (x_0,t_0) to (x,t).

The Feynman propagator is an integral over all quantum paths starting from x_0 at t_0 and finishing in x at time t. These paths are weighted with the exponential factor *iS* in units of ħ. In case of strong laser fields this is a strongly oscillating function, so only the neighborhood of those quantum paths contribute to the integral, where the phase, and so the action S, is stationary. This condition of stationary action defines the trajectories of particles in classical mechanics. Therefore we can approximate the momentum obtained by the particles in the field E(t) given by Eq. (2) by the classical momentum p where A(t) is the pulse envelope, ω_0 the center radial frequency of the laser pulse, $\vec{x}$ and $\vec{y}$ two orthogonal unit vectors in the plane of polarization, and ε describes the ellipticity and helicity of the pulse, where $|\varepsilon| \le 1$.

$$E(t) = A(t)(\sin(\omega_0 t)\cdot\vec{x} + \varepsilon\cdot\sin(\omega_0 t)\cdot\vec{y}). \tag{2}$$

The classical momentum, the electron gains in the laser field is given in Eq. (3).

$$\begin{aligned} p &= \int_{t_i}^{\infty} F(t)\,dt = -e\int_{t_i}^{\infty} E(t)\,dt \\ &= -e\int_{t_i}^{\infty} A(t)\left(\sin(\omega_0 t)\cdot\vec{x} + \varepsilon\cdot\cos(\omega_0 t)\cdot\vec{y}\right)dt \\ &= -\frac{e}{\omega}\left[-A(t)\cos(\omega_0 t)\vec{x} + \varepsilon\cdot A(t)\sin(\omega_0 t)\vec{y}\right]_{t_i}^{\infty} + \\ &\quad \frac{e}{\omega}\int_{t_i}^{\infty} (\tfrac{d}{dt}A(t))\left(-\cos(\omega_0 t)\cdot\vec{x} + \varepsilon\cdot\sin(\omega_0 t)\cdot\vec{y}\right)dt \\ &\approx \frac{e}{\omega}\left(A(t_i)\cos(\omega_0 t_i)\vec{x} - \varepsilon\cdot A(t_i)\sin(\omega_0 t_i)\vec{y}\right), \end{aligned} \tag{3}$$

where t_i is the instant of ionization. The approximation in Eq. (3) assumes a slowly varying pulse envelope that allows us to set the time derivative of the envelope to zero and neglect the last integral term in line 4 of Eq. (3). This approximation work extremely well even for few cycle laser pulses: A numerical comparison of this approximation with the exact result leads to a maximal error of the order of 7.5% of the maximum momentum for a 5.9-fs Gaussian, Fourier-limited laser pulse with a center wavelength of 780 nm. For a perfect circularly polarized pulse with $\varepsilon = 1$, Eq. (3) implies that the final momentum shows a 90 - degree phase shift compared to the direction of the electric field of the pulse at the instant of ionization. This means that the maximum of the final momentum distribution is rotated by 90 degrees from the direction of the maximum electric field. The final momentum distribution depends on the ellipticity but can be calculated in a straightforward way as well. The temporal trajectory can be determined by numerical integration and is shown in Fig. 1 (Media 1).

#129004 - $15.00 USD Received 25 May 2010; revised 23 Jul 2010; accepted 23 Jul 2010; published 2 Aug 2010

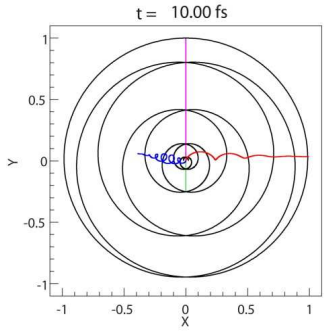

Fig. 1. (Media 1). Classical spatial trajectories in a perfect circularly polarized laser beam (i.e. ε = 1). Blue: Trajectory of an electron ionized 2.5 cycles before reaching the maximal intensity. Green: Direction of field at instant of ionization for purple trajectory. Red: Trajectory of an electron ionized at the instant of maximal intensity. Purple: Direction of field at instant of ionization for red trajectory. Black: Path of the electric field vector of a 5.9-fs Gaussian pulse in the range of ± 10 fs. (2663K)

Within this model, the moment of ionization of a detected electron can be determined by inversion of Eq. (3). It is crucial for an unambiguous inversion of the momentum-to-time mapping that the electric field is well known and that the ionization is essentially restricted to half a laser period centered around the field maximum in the case of linear polarization or to a full laser cycle in the case of circular polarization. As discussed above, a classical model for the electron propagation can be expected to work very well. Such models provide intuitive understanding of the resulting momentum distribution. They explain the offset of approximately 90 degrees between the direction of the maximum of the electric field and the direction of the maximum of the momentum distribution in the case of circularly polarized light (see Eq. (3)), or the origin of the knee structure in the double ionization rate in the case of linearly polarized light [3]. They also offer the possibility to investigate the influence of different parameters very quickly. While the driving of a continuum electron by the laser field can be estimated classically, the ionization process itself is a fundamental quantum mechanical process. The description of this process in this semiclassical model needs to be obtained by a different theory such as the ADK-Theory [11] for the tunnel ionization. In principle, all aspects of strong field processes can be investigated by solving the time dependent Schrödinger Equation (TDSE), but the main drawback is the large computational effort. The computational time requirements tend to impose feasibility limits in the investigation of different origins of an effect appearing in the calculation.

In the next two sections we show in more detail how to combine the ADK-Theory with classical motion to obtain the momentum distributions for ionization of helium by elliptically polarized ultrashort intense laser pulses under experimental conditions. Section two describes the generation and characterization of a very broadband elliptically polarized laser pulse in the one to two optical cycle regime. The fully characterized electric field is then used in section three to calculate the momentum distributions in the case of single ionization of helium using the semiclassical model described above, followed by comparison of the results with experiment. Section four discusses the limitations of the semiclassical model.

2. Full characterization of elliptically polarized field

In the classical picture given above for a perfect circularly polarized laser pulse the time of ionization during one laser cycle is mapped into momentum space onto a torus while ionization in linearly polarized light maps the time of ionization onto a cigar like structure. The variation of the amplitude of the electric field in the case of circular polarization is governed by the envelope of the laser pulse, while the variation of the total amplitude in the

#129004 - $15.00 USD Received 25 May 2010; revised 23 Jul 2010; accepted 23 Jul 2010; published 2 Aug 2010

case of linear polarization is governed by the rapidly oscillating laser field at the carrier frequency. As a consequence, the variation of the ionization rate on the time scale of one laser cycle is much smaller for circular than for linear polarization, where the ionization rate follows the oscillations of the intensity with twice the carrier frequency. This leads to different statistics in the momentum distribution: while the momentum distribution is equally populated over the whole torus for circular polarization, the distribution shows a peak at zero momentum for linear polarization. From an experimental point of view, inverting the time-to-momentum mapping is more robust for circular polarization since the statistic is equally distributed as a function of angle. In reality however it is very difficult to obtain perfect circular polarization for pulses in the two-optical-cycle regime. To create perfect circularly from linearly polarized light, it would have to be split into two perpendicularly polarized pulses, where one of these pulses has to accumulate a $\pi/2$ phase shift for each frequency component in its spectrum. The most common tools for creating circular polarized light are the $\lambda/4$ retardation plates and Fresnel rhombs. The Fresnel rhombs are not suitable for ultrashort laser pulses, since the pulse travels through a few centimeters of highly dispersive material which requires many higher orders of dispersion compensation. In addition, the phase shift difference acquired between the two perpendicularly polarized laser pulses is frequency dependent. The same is true for retardation wave plates, but the amount of dispersive material can be reduced to the order of one millimeter. This approach was chosen by Eckle et al. [7] in their experimental setup, and this approach will be discussed in more details in this section. Recently dispersion-free reflective phase retarder have been developed [12], the coating design is optimized to avoid dispersion and the retardation error is in the same order like for achromatic retardation plates. This approach will reduce the effort to compensate dispersive material, the retardation error will sill introduce a for ionization experiments significant amount of ellipticity.

In the case of linearly polarized pulses, the electric field can be measured using FROG [13] or SPIDER [14] and the CEO phase can be measured using for example the stereo – ATI [5]. Eckle et al. [7] have shown that in case of circular polarized light, the CEO phase can be retrieved from the momentum distribution, but there is no direct way to characterize the electric field of an elliptically polarized pulse. In general, the generation of ultrashort, amplified CEO-phase stable laser pulses centered around 800 nm usually involves the compression with a hollow core fiber [15] or with filamentation [16]. Typically, the spectrum has a bandwidth of a few hundred nanometers, and the pulse exhibits a rather complex pulse shape which is far from an ideal Gaussian or sech^2 pulse. Therefore the exact dispersion of the material of the retardation plate has to be taken into account. There are no single birefringent materials which show the desired retardation properties over a sufficient bandwidth. Therefore a combination of materials is being used for optimal dispersion compensation, which are referred to as achromatic retardation plates. In the visible and near-infrared regime they consist of a combination of MgF_2 and quartz. This also yields a small difference in group velocity and group delay dispersion (GDD) along the ordinary and extraordinary axes. The use of quartz complicates the propagation of the pulse through the retardation plate: G. Szivessy and Cl. Münster [17] show that the optical activity of quartz does not vanish for propagation perpendicular to the crystal axis, as commonly used in retardation plates. This leads to elliptical eigenmodes of the quartz plate, which are being rotated by the non-optically active MgF_2 plate. The eigenmodes of the combination of both parts of the retardation plate are elliptical and the orientation of the major axes changes with wavelength. To calculate the electric field behind the retardation plate, the optical activity of quartz and the dispersion of quartz and MgF_2 have to be taken into account. The calculation of the propagation through the retardation plate is performed in two steps. First, the linear pulse is being propagated along one of the axis of the retardation plate. This step takes care of the dispersion of the pulse and ignores the effect of optical activity. Second, the stretched pulse is Fourier transformed, split into polarization eigenmodes (Eq. (4) and Eq. (5)) P1 and P2 and for each frequency component a frequency dependant phase shift δ is acquired.

#129004 - $15.00 USD Received 25 May 2010; revised 23 Jul 2010; accepted 23 Jul 2010; published 2 Aug 2010

$$P_1 = \begin{bmatrix} \cos(\alpha) & -\sin(\alpha) \\ \sin(\alpha) & \cos(\alpha) \end{bmatrix} \begin{bmatrix} \frac{1}{\sqrt{1+\varepsilon^2}} \\ i\frac{\varepsilon}{\sqrt{1+\varepsilon^2}} \end{bmatrix}, \tag{4}$$

$$P_2 = \begin{bmatrix} \cos\left(\alpha+\frac{\pi}{2}\right) & -\sin\left(\alpha+\frac{\pi}{2}\right) \\ \sin\left(\alpha+\frac{\pi}{2}\right) & \cos\left(\alpha+\frac{\pi}{2}\right) \end{bmatrix} \begin{bmatrix} \frac{1}{\sqrt{1+\varepsilon^2}} \\ i\frac{-\varepsilon}{\sqrt{1+\varepsilon^2}} \end{bmatrix}. \tag{5}$$

The major challenge for this model of the propagation is the limited information about the exact dispersion data and about the optical activity parameters of quartz [17–19]. We fitted the available data for quartz [20] in the wavelength range from 404 to 1160 nm with the Sellmeyer equation (Eq. (6) and Table 1.), which we used for the first propagation step in combination with the dispersion formulas given by Dodge et al. [21] for MgF_2. The necessary data for the second propagation step through the retardation plate used by Eckle et al. [7] has been kindly provided by its manufacturer Bernhard Halle Nachfolger GmbH and are shown in Fig. 2.

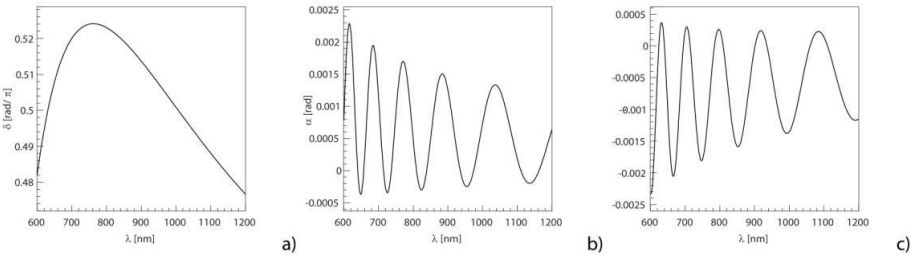

Fig. 2. Parameters of the λ/4 waveplate: a) Phaseshift δ, b) rotation angle α of the eigenmodes, c) ellipticity parameter ε.

$$n_i^2 - 1 = \sum_{j=1}^{6} \frac{A_j \lambda^2}{\lambda^2 - \lambda_j^2}. \tag{6}$$

Table 1. Parameters in Eq. (6)

	$\mathbf{n_o}$	$\mathbf{n_e}$
$\mathbf{A_1}$	0.34418	0.34057
$\mathbf{A_2}$	0.33846	0.33721
$\mathbf{A_3}$	0.33487	0.3486
$\mathbf{A_4}$	0.33949	0.35784
$\mathbf{A_5}$	6.64134	6.59729
$\mathbf{A_6}$	6.8756	6.66729
$\boldsymbol{\lambda_1}$	0.00514	0.00515
$\boldsymbol{\lambda_2}$	0.00531	0.00532
$\boldsymbol{\lambda_3}$	0.054	0.00533
$\boldsymbol{\lambda_4}$	0.01558	0.015792
$\boldsymbol{\lambda_5}$	1166.36478	1091.96331
$\boldsymbol{\lambda_6}$	1192.17287	1106.31822

#129004 - $15.00 USD Received 25 May 2010; revised 23 Jul 2010; accepted 23 Jul 2010; published 2 Aug 2010

The spectrum of the pulse used by Eckle et al. [7] extends the region of the supplied data to shorter wavelength by 50 nm. This region contains 2.5% of the pulse energy, so the error introduced by cubic spline extrapolation of the retardation plate specifications into this region will not lead to a significant amount of error, especially since the parameter with strongest impact on the electric field δ shows a smooth behavior and can safely be extrapolated. The resulting pulse has a FWHM of 5.9 fs and exhibits a time dependent ellipticity as shown in Fig. 3. The ellipticity becomes visible as a wave-like modulation on a smooth pulse envelope. The position in time of the maxima in the modulation changes as a function of the CEO phase of the pulse. This results from the combination of the rotation of the direction of the electric field of the entire pulse due to the change of the CEO phase, and the fact that the axes of the polarization are fixed in laboratory frame by the position of the retardation plate. The time-dependent ellipticity can be expressed by the quotient of the axes of the polarization ellipse by the use of the Stokes parameter [22]. The ellipticity lies between 5 and 10 percent in the region of ± 5 fs around the pulse center as shown in Fig. 3.

3. Final momentum distribution using ADK rate and Newtonian motion

As shown by Eckle et al. [7], ellipticity changes the CEO-dependent behavior of the electron momentum distribution. The maximum flips from one lobe of the distribution to the other, see Fig. 4, instead of the smooth rotation expected for perfect circular polarization. The rotation expected for an ideal circular pulse is seen only after the momentum distribution is divided by a CEO phase-averaged distribution (Fig. 4). In this section, we introduce a simple method for calculating electron momentum distributions that reproduces the effects measured by Eckle et al. [7]. We combine the ADK tunnel theory with classical 2D particle propagation in the calculated field from section one to obtain the momentum distributions. The classical propagation is done in velocity space since only the particle momentum can be obtained from the experimental data, which also reduces the computational time. To match the quantum mechanical momentum distribution we use the predictions of the extended ADK theory [23]. If not stated otherwise, atomic units are used throughout the paper. Within this approach, the ionization rate w_s for circular polarized, stochastic light [23] is given by Eq. (7):

$$w_s \sim \exp\left(-\frac{3^{\frac{1}{3}}}{E^{\frac{2}{3}}}\left[2\varepsilon_i + p_\perp^2 + (p_\parallel - \frac{E^*}{\omega})^2 \right] \right) \text{ with } E^* = E^{\frac{2}{3}}(2\varepsilon_i)^{\frac{1}{2}} 3^{-\frac{1}{3}}. \qquad (7)$$

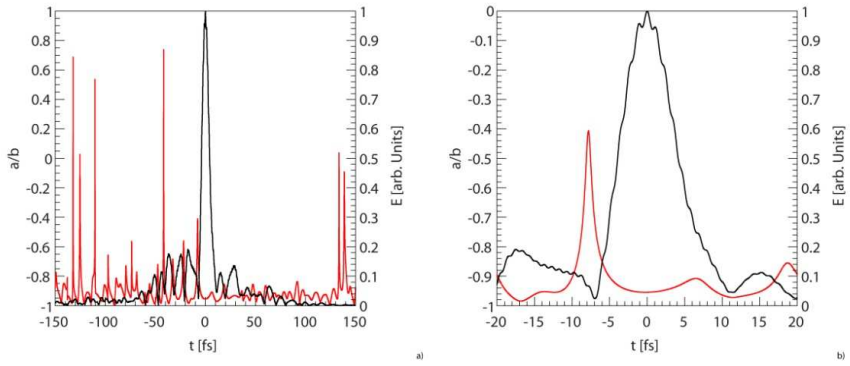

Fig. 3. a) Pulse shape (black curve, right scale) and ellipticity (red curve, left scale). b) zoom into central region of a). We used a typical pulse shape of the electric field of the laser pulses from experimental data. The time dependent ellipticity is expressed as the ratio of the two major axis of polarization; the sign represents the helicity.

#129004 - $15.00 USD Received 25 May 2010; revised 23 Jul 2010; accepted 23 Jul 2010; published 2 Aug 2010

where E is the electric field strength, ε_i the ionization potential and ω the angular frequency of the laser light. Delone and Krainov used $p_\parallel$ as the final momentum of the electron in the polarization plane and $p_\perp$ as the final electron momentum perpendicular to it. This extension provides a momentum distribution along and perpendicular to the polarization directions for non-monochromatic circularly polarized light. Since we ignore the Coulomb potential and the spatial dependence of the electric field in our semiclassical model, the initial momentum distribution, centered at momentum 0 is transferred into the final momentum distribution by an offset equal to the momentum gained by the electron on its classical trajectory. To adapt the momentum distribution of Eq. (7) for an instantaneous ionization, we change the interpretation of $p_\perp$ to the momentum perpendicular to the electric field vector at the instant of ionization. In tunneling theories the electron has zero velocity after tunneling through the potential barrier. We therefore shift the distribution of $p_\parallel$ by E^*/ω to zero. We use this adapted momentum distribution to provide initial conditions for the classical trajectories starting at t_i with an electric field strength $E = E(t_i)$. Momentum frequency distributions are created for all distributions numerically using the acceptance–rejection method. Substituting the shifted $p_\parallel$ in Eq. (7), this equation can be written as a product of three exponential functions, each of them depending either on the ionization potential, the shifted $p_\parallel$ or $p_\perp$, showing the statistical independence of this quantities. Motivated by this independence we used Eq. (7) for the momentum distribution and the ionization rate was calculated by the ADK-formula for circularly polarized light [11].

The propagation of the electron after it has tunneled through the potential barrier is modeled by solving numerically the equation of motion in the electric field of the laser pulse by the Runge-Kutta 4th order method [24] in velocity space. We have used equally spaced instants of ionization in the time interval ± 5 fs in time steps of 0.01 fs around the center of the laser pulse. The ionization probability outside this time interval can be neglected for a 5.9 fs laser pulse with the intensity of 3.92 10^{14} W/cm^2. The electron is then propagated in the electric field with no spatial dependency up to 200 fs after the pulse center. To match the experimental ion data, the temperature of the gas target of 2.8 K was taken into account by adding a velocity according to the Maxwell distribution. The final velocity is transformed to momentum and this value is then stored in a histogram weighted by the ADK Rate of the electric field at the instant of ionization, assuming that the ADK Rate for circularly polarized light is still a good approximation for the ionization rate of the elliptically polarized pulse with an ellipticity of about 0.9. For each starting time 400 trajectories have been computed, which can be done efficiently by calculating the propagation only once for each starting point and then calculating the initial and thermal velocities independently for each trajectory, since these velocities represent just an offset of the trajectory in velocity space. The intensity is used as a fitting parameter to the experimental data. The best fit was achieved at an intensity of 3.92 10^{14} W/cm^2 resulting in a Keldysh parameter γ gamma of 1.14, which is well within the experimentally estimated values. The use of tunneling based theories for $\gamma > 1$ has been successfully shown by Uiberacker et al. [25]. Our model yields excellent agreement with the experimental data of Eckle et al. [7]. It reproduces the general behavior of shifting the intensity from one lobe of the distribution into the other not only qualitatively but also quantitatively as shown in direct comparison of the measured and calculated angular distributions (Fig. 4).

#129004 - $15.00 USD Received 25 May 2010; revised 23 Jul 2010; accepted 23 Jul 2010; published 2 Aug 2010

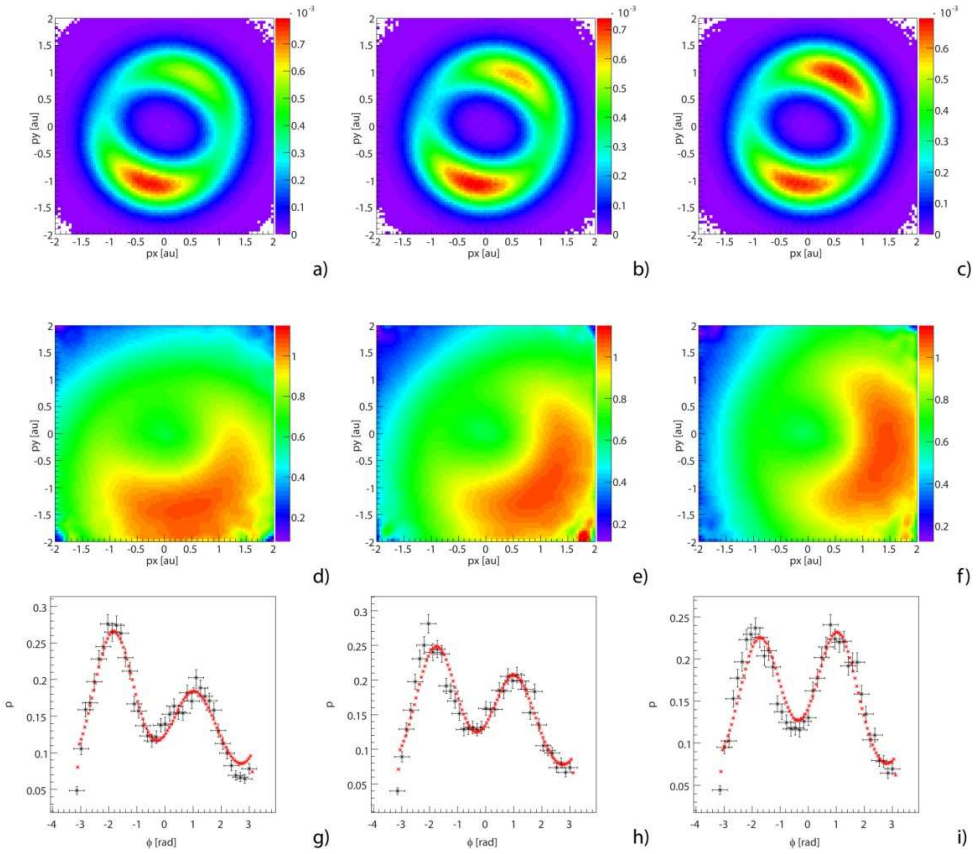

Fig. 4. a) to c): Helium ion momentum distribution, ionized at 3.92 10^{14} W/cm^2. d) to f): as a) to c) but smoothed and normalized with respect to a smoothed distribution with random CEO phase. Panels g) to h): Helium ion angular distribution, comparison theory and experiment: Red - theory, black – experiment [7]. Distributions in each row have the same CEO – phase and the increment between the rows is 0.497 radian.

4. Limitations

For intensities, where depletion of the ground state can be neglected, and the ionization takes place mainly at the peak intensity in the laser field, the laser pulse can be modeled with a Gaussian pulse with the ellipticity in the center of the calculated pulse. This approach is no longer valid, once depletion has to be taken into account [26]. The momentum distribution is strongly influenced by the shape of the laser pulse at the time of ionization, and the ellipticity varies strongly outside the central region of the pulse, as seen in Fig. 3. This effect is illustrated in Fig. 5, showing the different angular momentum distributions calculated using ADK rates for ionization of xenon for circularly polarized light and propagation in a Gaussian pulse at 10^{16} W/cm^2. This picture shows only the general behavior, since in this intensity region, where the peak intensity is far above the over-barrier intensity, the ADK rates are no longer valid. Since the ground state can be depleted almost completely within half a laser cycle, see Fig. 5, more accurate rates are needed for a quantitative calculation. Empirical formulas for the static field ionization rates are known for several elements [27] in the barrier-suppression regime, but the comparison of the ionization probability calculated from these rates and from TDSE calculations shows a significant deviation [27].

#129004 - $15.00 USD Received 25 May 2010; revised 23 Jul 2010; accepted 23 Jul 2010; published 2 Aug 2010

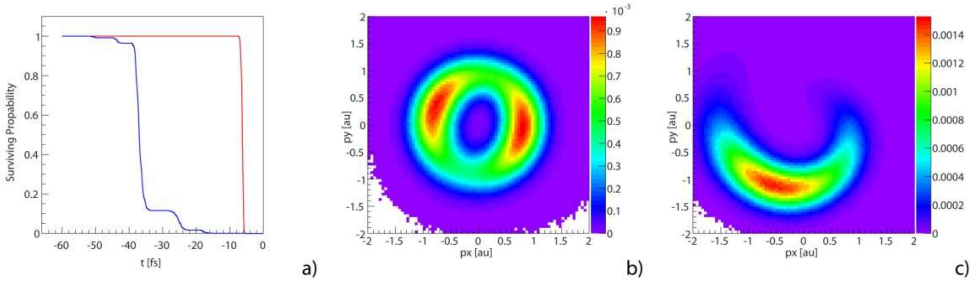

Fig. 5. a): Surviving probability of Xenon for CEO phase stabilized, elliptically polarized laser pulse, FWHM of 5.9 fs and a peak intensity 1 10^{16} W/cm^2. Result for measured pulse (blue) and for a Gaussian pulse matching ellipticity, CEO phase and wavelength of the measured pulse (red). Resulting momentum distribution for the measured pulse b) and for the Gaussian pulse c).

We can neglect the momentum of the ionizing photons, and therefore momentum conservation between the ion and the electron is fulfilled. Thus the forces acting on the particles have the same magnitude and opposite directions. However a limitation of the model is becoming visible when the angular momentum is investigated. For a particle starting in the origin of coordinates with velocity zero the angular momentum L is given by:

$$\vec{L} = \vec{r} \times \vec{p} = \int_{t_i}^{t_f} \int_{t_i}^{t} \frac{q \cdot \vec{E}(\tau)}{m} d\tau dt \times \int_{t_i}^{t_f} q \cdot \vec{E}(\zeta) d\zeta = \frac{q^2}{m} \int_{t_i}^{t_f} \int_{t_i}^{t} \vec{E}(\tau) d\tau dt \times \int_{t_i}^{t_f} \vec{E}(\zeta) d\zeta. \qquad (8)$$

From the q^2 factor in Eq. (8) it follows that the angular momenta of ions and electrons have the same sign and the numerical analysis of this equation shows that L cannot be assumed to be zero. As a consequence the angular momentum has to be provided by the electric field. The time dependence of L and the kinetic energy of the system of ion and electron show two striking features in Fig. 6. The amount of photons needed to provide the kinetic energy is different from the amount of photons needed to provide the angular momentum. The second feature is that the trend is not correct: In the region where the magnitude of the total angular momentum reaches its maximum between its second and third zero crossing, the kinetic energy is continuously increasing. There is a region where the magnitude of the total angular momentum decreases but the total kinetic energy increases. A decrease of angular momentum could be only due to emission of photons while an increase of kinetic energy indicates an absorption of photons. As long emission of low energy photon is excluded, this leads to a contradiction in terms of quantum mechanics. Its origin is the description of the laser field: One could theoretically produce the electric field used in Eq. (3) by a plate capacitor which rotates with frequency ω_0 while the electric field inside the capacitor has the amplitude $A(t)\cdot(\cos^2(\omega_0 t) + \varepsilon\cdot\sin^2(\omega_0 t))^{1/2}$. This external plate capacitor will enforce the angular momentum conservation in a classical picture.

The electric field used in equation Eq. (3) can also be interpreted as the dipole approximation of a laser field, which is usually treated as the solution of the source free Maxwell equation. Classically is not clear how angular momentum conservation can be fulfilled in an electric field having no sources. Newton's third law of motion cannot be fulfilled since there is only one classical particle feeling a force.

One should notice, that by changing the inertial frame to a frame moving with the final velocity of one of the particles and its origin matching the origin of the original frame at the time of ionization the particles initial and final angular momentum vanishes. Since the velocities of the electron and the ion are different, this condition cannot be fulfilled simultaneously for both particles. So even asymptotic angular momentum conservation for $t = \pm\infty$ is not fulfilled.

#129004 - $15.00 USD Received 25 May 2010; revised 23 Jul 2010; accepted 23 Jul 2010; published 2 Aug 2010

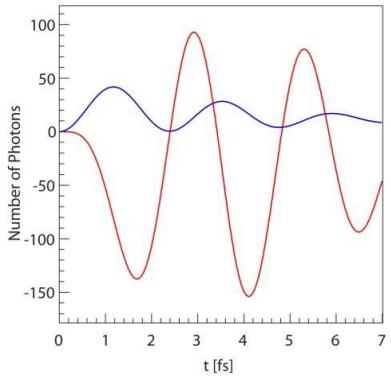

Fig. 6. Total angular momentum in units of ħ (red line) and total kinetic energy (blue line) in units of h·υ for the system of an electron and a Helium ion, ionized at t = 0 with a 5.9-fs Gaussian pulse shape and a peak intensity of 4 10^{14} W/cm^2.

5. Summary

We have analyzed the propagation of an ultra broadband pulse through an achromatic retardation plate and used the calculated field for simulations of the expected momentum distributions. The excellent reproduction of the measured momentum distributions shows the validity of the classical approach to the propagation of the electrons in the laser field and supports the classical mapping of momentum to time. The simplicity and the speed of the computational approach make this method a valuable tool for estimating in advance the quality of the circularly polarized light to be used in experiments and its influence on momentum distributions in ionization experiments as long as depletion plays no role in the reaction, the intensity is below the over-barrier threshold and the angular momentum of single trajectories is not considered.

Acknowledgments

We thank Prof. Reiss, Adrian Pfeiffer, and Dr. Zinner from Bernhard Halle Nachfolger GmbH for fruitful discussions. This work was supported by the Studienstiftung des deutschen Volkes and by the NCCR Quantum Photonics (NCCR QP), research instrument of the Swiss National Science Foundation (SNSF).

#129004 - $15.00 USD Received 25 May 2010; revised 23 Jul 2010; accepted 23 Jul 2010; published 2 Aug 2010